

**REPUBLIC OF AZERBAIJAN**

*On the rights of the manuscript*

**ABSTRACT**

of the dissertation for the degree of Doctor of Science

**THE EFFECT OF CATION–CATION SUBSTITUTIONS ON  
THE FORMATION OF THERMAL AND OPTICAL  
PROPERTIES IN OPTICALLY ACTIVE CHALCOGENIDES**

|                   |                               |
|-------------------|-------------------------------|
| Specialty:        | 2211.01 – Solid State Physics |
| Field of Science: | Physics                       |
| Applicant:        | <b>Arzu Oruc Dashdemirov</b>  |

**Baku – 2025**

The work was performed at Baku State University and Azerbaijan State Pedagogical University.

**Official opponents:** - Doctor of physical sciences, professor  
**Ali Hasan Huseynov,**



- Doctor of physical sciences, professor  
**Rovnag Mirza Rzayev,**

- Doctor of physical sciences, professor  
**Musavar Abdussalam Musayev,**

- Doctor of physical sciences, professor  
**Mantig Bahadur Jafarov**

Dissertation Council ED 2.19 of Supreme Attestation Commission under the President of the Republic of Azerbaijan operating at Baku State University

Chairman of the Dissertation Council:

Doctor of physical sciences, associate professor  
**Huseyn Mikayil Mammadov**

Scientific secretary of the Dissertation council:

doctor philosophy in physics  
**Shahla Nabi Hajiyeva**

Chairman of the scientific seminar:

Doctor of physical sciences, associate professor  
**Sadiyar Soltan Rahimov**



## GENERAL CHARACTERISTICS OF THE WORK

**Relevance of the topic and degree of elaboration.** The dissertation is devoted to the study of the thermal and optical properties of optically active chalcogenides. It is well established that chalcogenide semiconductors exhibit a range of remarkable physical properties. Partial substitution of either the metallic atoms or the chalcogen atoms in these compounds leads to modifications in both the crystal and electronic structures, which in turn alter the overall physical-chemical properties of the system. By applying partial atomic substitution methods, it is possible to control the physical characteristics of the samples. Therefore, in recent years, extensive research in this direction has been carried out. It has been shown that substitution with rare-earth elements results in the emergence of interesting optical properties in the newly obtained materials. Thus, introducing rare-earth elements into chalcogenide semiconductors with well-established structural and optical properties makes it possible to observe new effects. This is particularly significant, as chalcogenide semiconductors are regarded as highly active materials both electrically and optically.

It is also known that temperature induces various changes in solids. With increasing thermal energy, the amplitude of lattice vibrations grows, leading to modifications in the thermodynamic state of the system as a whole. In semiconductors, a rise in temperature increases the concentration of free charge carriers, which directly influences their electrical and optical properties. Therefore, studying the properties of solids as a function of temperature is important not only for investigating their thermal properties but also for understanding the general processes occurring in the system. The study of phase transitions in solids is of particular importance, as the state of the system changes after a transition: many physical properties observed in the previous phase disappear, while new ones emerge. In solids, transitions such as ferroelectric–paraelectric, ferromagnetic–antiferromagnetic, and semiconductor–metal transitions can occur. For this reason, the study of temperature-induced processes in solids

and the mechanisms of variation of thermodynamic parameters and functions is highly significant.

The  $\text{Cu}_2\text{Se}$  and  $\text{GeS}$  systems have long been investigated due to their interesting physical properties. In copper- and silver-containing semiconductors, the processes of phase formation and transformation have been studied in sufficient detail. It has been established that under the influence of temperature, these compounds form structures of higher symmetry. It is also known that cation–cation and anion–anion substitutions give rise to differences in the crystal and electronic structures, since differences in ionic radii affect interatomic distances. The substitution of rare-earth elements in  $\text{Cu}_2\text{Se}$  crystals is of particular interest, as the ionic radii of lanthanides are significantly larger than those of copper atoms. This difference results in lattice strain in the unit cell, which in turn affects the other properties of the crystals. Although such effects have been studied in many systems, they remain unexplored in copper-based chalcogenides, particularly in  $\text{Cu}_2\text{Se}$  crystals.

Layered  $\text{GeS}$  crystals occupy a special place among semiconductors. Their structural characteristics, optical and electrical properties, and radiation resistance have been studied for many years. It has been established that substitution of germanium with rare-earth elements leads to the formation of structural defects due to differences in ionic radii, and that these defects can be recombined under ionizing radiation. While such structural modifications have been investigated, the optical and thermal properties of these samples have not yet been fully clarified. At elevated temperatures, structural defects in solids can recombine, and such processes may induce phase formation and structural transformations under the influence of thermal energy. Therefore, studying the thermal properties of these systems at high temperatures is important not only for understanding the effects of cation–cation substitutions but also for revealing the thermophysical processes occurring under thermal excitation.

Investigations of  $\text{Cu}_2\text{Se}$  and  $\text{GeS}$  compounds have shown that the effects arising from cation–cation substitutions, particularly with regard to their optical and thermal properties, require further

systematic study. In this dissertation, systems of the type  $\text{Cu}_{2-x}\text{Tm}_x\text{Se}$  and  $\text{Ge}_{1-x}\text{La}_x\text{S}$  ( $\text{La} = \text{Nd}, \text{Sm}, \text{Gd}$ ) were synthesized at various concentrations of rare-earth elements. The structures, optical, and thermal properties of the obtained systems were studied using modern methods, and the experimental data were analyzed with high precision through advanced software tools.

The dissertation was carried out at the Department of General Physics and Methods of Teaching Physics of the Faculty of Physics, Baku State University, and at the Faculty of Physics, Azerbaijan State Pedagogical University.

**Object and subject of the research.** The objects of the research are new compounds obtained on the basis of  $\text{Cu}_2\text{Se}$  and  $\text{GeS}$  chalcogenide semiconductors. These compounds were synthesized by substitutions with different atoms and at various concentrations. Single crystals of the systems  $\text{Cu}_{2-x}\text{Tm}_x\text{Se}$ ,  $\text{Ge}_{1-x}\text{Nd}_x\text{S}$ ,  $\text{Ge}_{1-x}\text{Sm}_x\text{S}$ , and  $\text{Ge}_{1-x}\text{Gd}_x\text{S}$  were grown, and depending on the features of the research method, samples were prepared for the investigation of their structural, thermal, and optical properties.

**Aim and objectives of the research.** The aim of the present dissertation is to obtain new functional compositions in chalcogenide semiconductors through cation–cation substitutions, to study the effects arising from differences in ionic radii of the substituted metal atoms, to investigate their optical and thermal properties, and to determine the mechanisms of processes observed in these systems under the influence of thermal energy.

In accordance with this aim, the following objectives were addressed:

- To synthesize single-phase layered  $\text{GeS}$  crystals through  $\text{Ge} \rightarrow \text{Ln}$  ( $\text{Nd}, \text{Sm}, \text{Gd}$ ) substitutions and to study the structural properties of the obtained layered crystals. To investigate the effect of the differences between the ionic radii of  $\text{Ge}$  and  $\text{Ln}$  atoms on crystallographic parameters and to determine the nature of defects in these crystals.
- To investigate the thermal properties of  $\text{Ge}_{1-x}\text{Ln}_x\text{S}$  crystals and to determine the mechanisms of variation of thermodynamic

parameters depending on the ionic radii and concentrations of the rare-earth elements.

- To study the shift of maxima in the photoconductivity spectra of GeS crystals substituted with Nd and Sm towards longer wavelengths with increasing temperature, and the corresponding decrease in photosensitivity.
- To reveal significant changes in the photoconductivity of GeS due to Ge  $\rightarrow$  Nd, Sm substitutions, including the appearance of additional maxima in the spectra at photon energies of  $E = 1.4$  eV and 1.3 eV within the temperature range  $200 \text{ K} < T < 250 \text{ K}$ .
- To synthesize  $\text{Cu}_{2-x}\text{Tm}_x\text{Se}$  ( $x = 0.1, 0.2, 0.3$ ) compounds, determine their rhombohedral R-3m (166) crystal structure, establish their crystallographic parameters, and analyze the structural aspects of Cu  $\rightarrow$  Tm substitutions.
- To investigate the thermal properties of  $\text{Cu}_{1.9}\text{Tm}_{0.1}\text{Se}$ ,  $\text{Cu}_{1.7}\text{Tm}_{0.3}\text{Se}$ , and  $\text{Cu}_{1.5}\text{Tm}_{0.5}\text{Se}$  compounds, to study the mechanisms of variation of thermodynamic parameters at high temperatures, and to determine the effect of cation–cation substitutions on thermal processes.
- To obtain the optical absorption and photoluminescence spectra of  $\text{Cu}_{2-x}\text{Tm}_x\text{Se}$  ( $x = 0.1, 0.2, 0.3$ ) compounds, to analyze the spectra in order to determine optical activity depending on Tm concentration, to establish the band gap energy of each crystal, and to reveal the dependence of band gap variation on Cu  $\rightarrow$  Tm substitutions.

### **Research methods.**

Modern research methods were employed to study the structural, thermal, and optical properties of the research objects. X-ray phase analysis of the synthesized chalcogenide semiconductors was carried out using the X-ray diffraction method. This method is regarded as one of the most advanced tools for studying the structure of crystalline solids, performing phase analysis, and obtaining detailed information on the crystallographic parameters of compounds. Compared with other diffraction methods, one of its main advantages is the possibility

of performing investigations on relatively small-scale samples under laboratory conditions. Using this method, the structural characteristics and crystallographic parameters of powdered samples were determined.

The thermal properties of the samples were studied using the **Differential Scanning Calorimetry (DSC)** method. This technique allows the determination of many thermodynamic parameters of materials at both high and low temperatures, providing insight into their physico-chemical characteristics. It is widely used to identify processes such as water release, decomposition, evaporation, oxidation, phase transitions, and melting. One of its main advantages is the ability to determine thermodynamic functions and calculate thermodynamic parameters based on the temperature dependence of the heat flow function by applying geometrical methods.

To provide a more detailed and comparative study of the thermal properties of the synthesized compounds, the **Thermogravimetric Analysis (TGA)** method was employed. This method makes it possible to study thermal transitions and physical processes observable through thermal excitation by analyzing changes in mass as a function of temperature. Sharp increases or decreases in mass observed during decomposition, evaporation, and oxidation processes are reflected in TGA spectra. For accurate calculation of thermodynamic parameters, not only the heat flow through the sample but also the sample mass at the corresponding point must be known. Therefore, in solid-state physics and thermodynamics, the combined use of DSC and TGA methods is considered most appropriate.

For the analysis of experimental data, various software tools and computational methods were applied. X-ray diffraction spectra were processed using the **Rietveld method** with the FullProf software package. The crystal structures of the newly synthesized compounds were modeled in three dimensions and their crystallographic parameters calculated using *DIAMOND 3.2*. For the determination of parameter dependencies, as well as for plotting and analyzing DSC and TGA spectra, *Origin 8 (2016 version)* was employed.

Optical studies were carried out using **Raman spectroscopy**. Employing different excitation wavelengths, both photoluminescence and excitation spectra of the various compounds were obtained at room temperature, providing comprehensive information about their optical properties.

**Main provisions submitted for defense:**

1. Synthesis of new compounds through partial substitution of Ge atoms with rare-earth elements (Nd, Sm, Gd) in layered GeS crystals and determination of their crystal structure.
2. Thermophysical properties of  $\text{Ge}_{1-x}\text{Ln}_x\text{S}$  compounds at high temperatures and the thermal transitions observed in the samples depending on the rare-earth element.
3. Observation of a phase transition (solid-to-liquid) in the  $\text{Ge}_{0.99}\text{Nd}_{0.01}\text{S}$  layered crystal at  $T = 596\text{ }^\circ\text{C}$ .
4. In GeS crystals obtained by  $\text{Ge} \rightarrow \text{Nd}$  cation–cation substitution, the appearance of additional maxima in the photoconductivity spectrum at photon energy  $E = 1.4\text{ eV}$  within the temperature range  $200\text{ K} < T < 250\text{ K}$ , explained by the dissociation of exciton–impurity complexes.
5. The photoluminescence spectrum of the  $\text{Ge}_{0.99}\text{Gd}_{0.01}\text{S}$  compound is associated with the  $6\text{P}_j \rightarrow 8\text{S}_j$  transition of gadolinium atoms ( $\text{Gd}^{3+}$ ,  $4f-4f$  transition).
6. Crystal structure of  $\text{Cu}_{2-x}\text{Tm}_x\text{Se}$  ( $x = 0.1, 0.2, 0.3$ ) compounds corresponds to the rhombohedral system with space group  $R-3m$  (166).
7. In the thermal spectra of  $\text{Cu}_{1.9}\text{Tm}_{0.1}\text{Se}$ ,  $\text{Cu}_{1.7}\text{Tm}_{0.3}\text{Se}$ , and  $\text{Cu}_{1.5}\text{Tm}_{0.5}\text{Se}$  compounds, a thermal effect observed at  $T = 140\text{ }^\circ\text{C}$  is attributed to the desorption of water molecules and the decomposition of hydroxide groups formed with Cu and Tm atoms.
8. Phase transition (solid-to-liquid) observed in  $\text{Cu}_{2-x}\text{Tm}_x\text{Se}$  ( $x = 0.1, 0.2, 0.3$ ) compounds at  $T > 600\text{ }^\circ\text{C}$ .
9. An absorption peak observed at  $\lambda = 320\text{ nm}$  in the absorption spectra of  $\text{Cu}_{2-x}\text{Tm}_x\text{Se}$  ( $x = 0.1, 0.2, 0.3$ ) compounds.

10. The band gap values of  $\text{Cu}_{2-x}\text{TM}_x\text{Se}$  compounds were determined as follows:  $E_g = 1.25$  eV for  $\text{Cu}_{1.9}\text{TM}_{0.1}\text{Se}$ ,  $E_g = 1.35$  eV for  $\text{Cu}_{1.8}\text{TM}_{0.2}\text{Se}$ , and  $E_g = 1.44$  eV for  $\text{Cu}_{1.7}\text{TM}_{0.3}\text{Se}$ .

### **Scientific novelty of the research:**

1. It was established that in crystals obtained by  $\text{Ge} \rightarrow \text{Ln}$  (Nd, Sm, Gd) substitution in layered GeS, the structures of compounds with up to 1% cation–cation substitution correspond to the orthorhombic system with space group Pnma.
2. The thermal properties of the  $\text{Ge}_{0.99}\text{Nd}_{0.01}\text{S}$  layered crystal were investigated within the temperature range  $25\text{ }^\circ\text{C} \leq T \leq 750\text{ }^\circ\text{C}$ . Thermal effects were observed at  $150\text{ }^\circ\text{C}$ ,  $181\text{ }^\circ\text{C}$ ,  $428\text{ }^\circ\text{C}$ ,  $480\text{ }^\circ\text{C}$ ,  $596\text{ }^\circ\text{C}$ ,  $671\text{ }^\circ\text{C}$ ,  $723\text{ }^\circ\text{C}$ , and  $760\text{ }^\circ\text{C}$ . It was determined that these thermal transitions correspond to processes such as decomposition, evaporation, and recombination of structural defects, accompanied by energy absorption.
3. At high temperatures, it was established that a phase transition occurs in the  $\text{Ge}_{0.99}\text{Nd}_{0.01}\text{S}$  layered crystal at  $T = 596\text{ }^\circ\text{C}$ , which corresponds to melting, i.e., the transition of the system from solid to liquid state.
4. In GeS crystals obtained through  $\text{Ge} \rightarrow \text{Nd}$  substitution, the maxima in the photoconductivity spectrum shift towards longer wavelengths with increasing temperature, indicating a decrease in photosensitivity. Additionally, an extra maximum was observed in the photoconductivity spectrum at  $E = 1.4$  eV within the temperature range  $200\text{ K} < T < 250\text{ K}$ , which was attributed to the dissociation of exciton–impurity complexes under the influence of heat.
5. In the photoluminescence spectra of GeS and  $\text{Ge}_{0.99}\text{Gd}_{0.01}\text{S}$  layered crystals in the wavelength range  $\lambda = 620\text{--}750\text{ nm}$ , a maximum was observed at  $\lambda = 685\text{ nm}$  for both compounds. The intensity of this maximum in  $\text{Ge}_{0.99}\text{Gd}_{0.01}\text{S}$  was several

times higher compared to GeS, explained by the  $6P_j \rightarrow 8S_j$  transition of gadolinium ( $Gd^{3+}$ ,  $4f-4f$  transition).

6. It was determined that the crystal structure of  $Cu_{2-x}Tm_xSe$  ( $x = 0.1, 0.2, 0.3$ ) compounds corresponds to the rhombohedral system with space group R-3m (166). An increase in lattice parameters was observed with increasing Tm concentration, explained by the difference in ionic radii between Tm and Cu atoms.
7. In the thermal properties of  $Cu_{1.9}Tm_{0.1}Se$ ,  $Cu_{1.7}Tm_{0.3}Se$ , and  $Cu_{1.5}Tm_{0.5}Se$  compounds, a thermal effect was observed at  $T = 140$  °C, attributed to the decomposition of hydroxide groups formed by adsorbed water molecules with Cu and Tm atoms.
8. Thermal analysis of  $Cu_{2-x}Tm_xSe$  ( $x = 0.1, 0.2, 0.3$ ) compounds revealed thermal effects associated with melting at  $T > 600$  °C. It was shown that the melting temperature decreases gradually with increasing Tm concentration.
9. The absorption spectra of  $Cu_{2-x}Tm_xSe$  ( $x = 0.1, 0.2, 0.3$ ) compounds were obtained, and optical activity depending on Tm concentration was determined. An absorption peak at  $\lambda = 320$  nm was observed experimentally, corresponding to the internal  $f-f$  electronic transition  ${}^3H_6 \rightarrow {}^1D_2$  of  $Tm^{3+}$  ions.
10. Based on absorption spectra, the band gap values of  $Cu_{1.9}Tm_{0.1}Se$ ,  $Cu_{1.8}Tm_{0.2}Se$ , and  $Cu_{1.7}Tm_{0.3}Se$  compounds were determined as  $E_g = 1.25$  eV,  $E_g = 1.35$  eV, and  $E_g = 1.44$  eV, respectively. It was established that the band gap increases with increasing Tm concentration in the crystals.

### **Theoretical and practical significance of the research.**

Chalcogenide semiconductors are materials of great importance in solid-state physics. The study of physical processes occurring in these compounds is crucial for explaining both electronic processes in solids and thermodynamic processes within the system. It is known that substitution of metal atoms alters the electronic configuration of semiconductors, which in turn may change the width of the band gap. Depending on the type of substitution, a semiconductor material may

even be transformed into a semimetal or metal. Therefore, such studies carry substantial scientific significance.

Under normal conditions, all solids are affected by temperature, and depending on the amplitude of atomic vibrations, various processes can occur. As temperature increases, these processes become more complex. Hence, the investigation of the thermal properties of such compounds at high temperatures provides baseline data for the explanation of many processes. In recent years, the importance of optically active materials in solid-state physics has increased, since they allow the study of electronic processes and the conversion of energy from one form to another.

The scientific significance of this dissertation is matched by the wide practical applicability of its results. Chalcogenide semiconductors are considered materials with broad application potential in modern electronics. Converters based on these materials retain their properties over long periods and remain operationally stable. High-temperature studies make it possible to evaluate their application potential, as many processes are accompanied by heating, which necessitates the use of converters capable of operating at elevated temperatures. In particular, in space technology, satellites, and aviation, the development of converters that can function under temperature gradients and maintain stability is essential. From this perspective, the results obtained in this research are of considerable importance.

It is also well known that current technological developments focus on creating optical devices that consume less energy. Thus, the synthesis and application of new optically active materials based on known compounds is highly necessary. In recent years, research efforts have increasingly focused on obtaining new optical materials by introducing rare-earth elements into semiconductor matrices. The results obtained in this work therefore hold significant promise for future applications in this field.

**Author's contribution.** The research objects were selected, synthesized, and prepared by the author in accordance with the research methods. The directions of the research and the objectives

were determined by the author, and the scientific significance of the expected results was foreseen. The author directly participated in the experiments and was the primary author of the scientific articles prepared and published in reputable peer-reviewed journals. The main results of the dissertation were presented by the author at scientific events of various scales.

**The reliability of the results presented** in the dissertation was ensured by the selection of research objects with wide application potential in modern electronics and device engineering, and by carrying out the investigations using new instruments with high precision. The results obtained were published in highly indexed peer-reviewed scientific journals, and these articles were cited by other scholars working in the field. The new scientific results were presented at international and national conferences and other academic forums, where they were repeatedly discussed before a wide audience of specialists and highly evaluated.

**Approbation and implementation.** The scientific results obtained were reported at the following national and international conferences:

- XXV International Scientific-Technical Conference and School on Photoelectronics and Night Vision Devices, Moscow, Russia, May 24–26, 2018.
- 7th International Conference “Modern Trends in Physics” (MTP-2021), Baku, Azerbaijan, December 15–17, 2021.
- 10th Rostocker International Conference: “Thermophysical Properties for Technical Thermodynamics”, Rostock, Germany, September 9–10, 2021.
- International Conference “Condensed Matter Research at the IBR-2”, Dubna, Russia, April 25–29, 2022.
- International Conference “Phase Transitions, Critical and Nonlinear Phenomena in Condensed Matter”, Makhachkala, Russia, September 10–15, 2023.
- 8th International Conference “Modern Trends in Physics”, Baku, Azerbaijan, November 30 – December 1, 2023.
- “Problems of Physics and Astronomy”, XXIV Republican Scientific Conference, Baku, Azerbaijan, May 17, 2024.

- “Actual Problems of Physics”, Republican Scientific Conference, Baku, Azerbaijan, November 29, 2024.
- “Physics of Metals and Alloys: Current Issues”, dedicated to the 50th anniversary of AzMIU, Baku, Azerbaijan, February 6–7, 2025.
- “The Role of Universities in the Development of Innovative Ecosystems”, ATU, Ganja, Azerbaijan, November 5–6, 2024.

**Publications.** The main findings of the dissertation have been published in 35 scientific works, including 23 articles (14 of which are indexed in the *Science Citation Index Expanded*) and 12 conference proceedings. The obtained results have also been included in the annual research reports of Baku State University and Azerbaijan State Pedagogical University.

**The total volume of the dissertation with a sign indicating the separate volume of the structural sections of the dissertation.**

The dissertation consists of an introduction, six chapters, conclusions, a list of 298 references cited in the work, and a list of abbreviations and symbols. Including 7 tables and 75 figures, the total length of the dissertation is 247 pages. Excluding figures, tables, and references, the total volume of the dissertation amounts to 333,681 characters. The distribution of characters by sections is as follows: Introduction – 38,799 characters; Chapter I – 86,712 characters; Chapter II – 40,887 characters; Chapter III – 44,883 characters; Chapter IV – 49,511 characters; Chapter V – 38,418 characters; Chapter VI – 30,857 characters; Conclusions – 3,614 characters.

## **BASIC CONTENT OF THE WORK**

In the *Introduction*, the relevance and degree of elaboration of the research topic, the main objectives of the dissertation, its scientific

novelty, theoretical and practical significance, as well as the goals and the main provisions submitted for defense are substantiated.

The *first chapter* of the dissertation is devoted to a literature review of the known properties of chalcogenide semiconductors established in previous studies. It is well known that chalcogenide semiconductors have long been the subject of research in solid-state physics. Their crystal structure, electronic structure, as well as electrical, thermal, and optical properties have been extensively investigated. The results obtained from studies of known compounds have been examined and presented. It has been established that the structural properties of semiconductors depend on both the metallic and chalcogen atoms. These changes are manifested not only in the crystal structure but also in structural phase transitions.

The crystal structure of the GeS compound was investigated using the X-ray diffraction method, and it was determined that its structure corresponds to the orthorhombic system with space group Pnma. The lattice parameters were identified<sup>1</sup> as  $a = 4.319(3) \text{ \AA}$ ,  $b = 3.651(4) \text{ \AA}$ , and  $c = 10.492(5) \text{ \AA}$ . To better illustrate the structure of GeS, its three-dimensional (3D) structure was modeled (Figure 1).

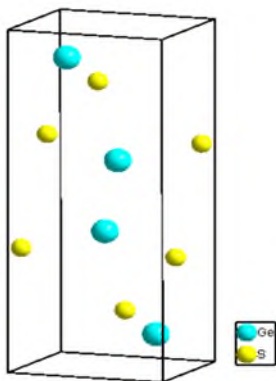


**Figure 1.** Crystal structure of the GeS compound.

---

<sup>1</sup> Alekperov, A.S. Effect of gamma irradiation on microstructure of the layered  $\text{Ge}_{0.995}\text{Nd}_{0.005}\text{S}$  / A.S.Alekperov, S.H.Jabarov, M.N.Mirzayev [et al.] // Modern Physics Letters B, – 2019. Mar.; v. 33, № 9, – p. 1950104-1-9.

As seen in the figure, sulfur atoms occupy positions both on the faces of the unit cell and throughout its volume, while germanium atoms are arranged diagonally across the unit cell and form covalent bonds with the sulfur atoms.

Among chalcogenide semiconductors, layered and chain-like structures are of particular importance. Their structural features significantly influence their physical properties. To investigate and analyze these properties, the results of previous studies on the Ge–X (X = S, Se, Te) systems were collected and analyzed. The structural differences observed in these systems depending on whether sulfur, selenium, or tellurium atoms are present were explained in terms of their ionic radii and electronic configurations. Information on the electronic structure and configuration of GeSe, GeS, and GeTe compounds was reviewed, providing detailed insight into their semiconducting properties.

In the study of crystals formed in the Ge–Se system, various structures were also observed. Similar to sulfur, selenium atoms form a range of compounds with germanium. Depending on the stoichiometric ratio of Ge and Se atoms, GeSe (divalent), GeSe<sub>2</sub> (tetravalent), or Ge<sub>4</sub>Se<sub>9</sub> (mixed valence) crystals may be obtained. X-ray diffraction studies of GeSe revealed that this compound crystallizes in orthorhombic symmetry with space group Pcmn, and lattice parameters<sup>2</sup>  $a = 4.38 \text{ \AA}$ ,  $b = 3.82 \text{ \AA}$ , and  $c = 10.79 \text{ \AA}$ . Thus, while GeS and GeSe semiconductors appear structurally similar, their structural properties differ, which can be attributed to differences between sulfur and selenium atoms and the compounds they form. To further explore the structure of layered germanium chalcogenide crystals, the Ge–Te system was also studied.

Investigations using X-ray and neutron diffraction established that the elements in the Ge–Te system exist in divalent states, leading to the synthesis of GeTe. Its crystal structure corresponds to the orthorhombic system with space group Pnma and lattice parameters a

---

<sup>2</sup> Jung-Eun, K., Yun, H. Reinvestigation of Ge<sub>4</sub>Se<sub>9</sub> based on single-crystal data // Acta Crystallographica Section C, – 2005. Aug.; v. 61, № 8, – p. 81-82

= 7.369 Å, b = 3.9249 Å, and c = 5.698 Å. However, during phase transitions, rhombohedral and cubic phases of higher symmetry were also observed.

The electrical properties of these layered chalcogenide crystals were analyzed, and the effects of temperature and radiation on these properties were examined. The optical properties of these compounds were also reviewed, with results obtained by different researchers using various methods. In the Ge–X (X = S, Se, Te) systems, the possibility of new physical properties emerging due to partial substitution of Ge atoms with other metallic atoms was also predicted.

In addition, the structural, electronic, electrical, thermal, and optical properties of copper chalcogenides were examined. Since copper atoms exhibit variable valence, the compounds that can be synthesized depend on the synthesis conditions and the stoichiometric ratios of the constituent elements.

In the Cu–S system, depending on the valence state of copper atoms, a variety of compounds may be formed, including Cu<sub>2</sub>S, CuS, Cu<sub>1.78</sub>S, Cu<sub>9</sub>S<sub>5</sub>, CuS<sub>2</sub>, Cu<sub>1.8</sub>S, Cu<sub>31</sub>S<sub>16</sub>, and Cu<sub>17</sub>S<sub>9</sub>. When copper is monovalent, Cu<sub>2</sub>S is formed, which crystallizes in hexagonal symmetry with space group P6<sub>3</sub>/mmc. X-ray structural studies determined the lattice parameters of Cu<sub>2</sub>S as a = b = 3.959 Å and c = 6.784 Å. In this hexagonal structure, copper atoms occupy two distinct positions: Cu1 at x = 0, y = 0, z = 0.25, and Cu2 at x = 0.2573, y = 0.5146, z = 0.4339. Sulfur atoms occupy the positions x = 0.6666, y = 0.3333, z = 0.25, forming covalent bonds with copper atoms<sup>3</sup>. The bond lengths were measured to lie within the ranged Cu–S = 2.2857–3.9591 Å.

At first glance, one might assume that the variable valence of copper atoms would result in lower structural symmetry. However, the results show that variable valence contributes to denser atomic packing, thereby giving rise to higher symmetry in the crystal structure. Similar to the Cu–S system, the Cu–Se system also exhibits

---

<sup>3</sup> Cava, R.J., Wuensch, B.J., Reidinger, F. Mobile ion distribution and anharmonic thermal motion in fast ion conducting Cu<sub>2</sub>S // *Solid State Ionics*, – 1981. Oct.; v. 5, – p. 501-504.

intriguing structural properties. Depending on the valence of copper, various compounds may be synthesized, including  $\text{Cu}_2\text{Se}$ ,  $\text{CuSe}$ ,  $\text{Cu}_{1.78}\text{Se}$ ,  $\text{Cu}_{0.87}\text{Se}$ ,  $\text{Cu}_3\text{Se}_2$ ,  $\text{CuSe}_2$ ,  $\text{Cu}_{1.95}\text{Se}$ ,  $\text{Cu}_{1.77}\text{Se}$ ,  $\text{Cu}_{1.89}\text{Se}$ , and  $\text{Cu}_{1.8}\text{Se}$ .

Among these,  $\text{Cu}_2\text{Se}$  is the most frequently encountered compound, and extensive information regarding its physical properties is available. Although it has been studied for a long time and its many physical-chemical properties are known, the analysis of prior results demonstrates the continued importance of further investigation of this compound. In particular, results of cation–cation and anion–anion substitutions were presented, and interesting thermal and optical properties were predicted for cases where copper atoms are replaced by rare-earth elements. At the end of the chapter, the open questions arising from these studies were identified, and the research topic selected by the author was substantiated.

*The second chapter* is devoted to the experimental methods employed in the research, the techniques used to analyze the data obtained, and detailed information about the instruments and equipment applied. High-precision, state-of-the-art instruments were used throughout the investigations.

The synthesis conditions of the selected compositions were predetermined, and the optimal parameters were established. X-ray phase and structural analyses of the obtained compounds were carried out. Using the X-ray diffraction (XRD) method, the lattice parameters, crystal system, and space group were determined. For the analysis of diffraction patterns, modern methods and computer software were employed. Infrared (IR) spectroscopy was used to study the atomic dynamics and lattice vibrations of the crystals.

The research samples were synthesized under high-vacuum conditions in high-temperature furnaces, following standard procedures for chalcogenide semiconductors. As starting materials, highly pure metals (Cu, Ge, Nd, Sm, Gd, Tm) and chalcogens (S, Se) were used in stoichiometric proportions. The mixtures were sealed in quartz ampoules of approximately 10–15 cm in length under a vacuum of  $10^{-3}$  mm Hg. The synthesis process was carried out in two stages:

in the first stage, the compounds were synthesized; in the second stage, single crystals were grown using the Bridgman method.

The crystal structure and phase composition of the synthesized compounds were studied using a **D8 ADVANCE diffractometer**. Powdered samples were examined at room temperature and under normal conditions using the X-ray diffraction method at 40 kV, 40 mA, with CuK $\alpha$  radiation ( $\lambda = 1.5406 \text{ \AA}$ ). The obtained diffraction patterns were analyzed by the **Rietveld method** using the *FullProf* software package.

The thermal properties of the compounds were investigated in a wide temperature range using **Differential Scanning Calorimetry (DSC)** and **Thermogravimetric Analysis (TGA)**. Measurements were performed with a **DSC3 STARe** device (Mettler Toledo) with temperature control achieved by MULTISTAR sensors. A standard adiabatic calorimeter was used in the range of 25 °C to 800 °C under an argon (Ar) atmosphere with a heating rate of 5°/min and gas flow rate of 20 ml/min. Cooling was carried out using the *NITROGEN UN 1977 SOFRIGERED LIQUID* analyzer system in combination with a digital temperature controller. The DSC and TGA spectra were analyzed using the *Origin* software.

Optical studies were performed using a **Raman spectrometer** (Tokyo Instruments, Inc.). Lasers with wavelengths  $\lambda = 532 \text{ nm}$ ,  $642 \text{ nm}$ , and  $785 \text{ nm}$  were used to obtain both photoluminescence and excitation spectra of the various compounds at room temperature. An **MS 3401 I monochromator** (SOL Instruments, Inc.) was also employed in the experiments.

For the analysis of X-ray diffraction spectra and determination of crystallographic parameters, several methods were applied. One approach is based on calculating lattice parameters from the interplanar spacing values ( $d_{hkl}$ ) of atomic planes, determined using Bragg's law:  $n\lambda = 2d_{hkl}\sin\theta$

Interatomic distances, in turn, allow the calculation of lattice parameters. For example, in hexagonal symmetry, the relation between interplanar spacing and lattice parameters is given by:

$$\frac{1}{d^2} = \frac{4}{3} \cdot \frac{h^2 + h \cdot k + k^2}{a^2} \cdot \left(\frac{l}{c}\right)^2, \quad (1)$$

where  $d$  is the interplanar spacing,  $h$ ,  $k$ ,  $l$  are Miller indices, and  $a$ ,  $c$  are the lattice parameters.

In the simplest case of cubic symmetry, the relation is:

$$1/d^2 = (h^2 + k^2 + l^2)/a^2. \quad (2)$$

Among the available methods, the Rietveld method<sup>4</sup> is considered the most accurate and widely used by crystallographers in recent years. Compared to other approaches, its advantage lies in the ability to extract more detailed information from diffraction spectra. In addition to determining crystal symmetry, space group, and lattice parameters, it also provides atomic coordinates (atomic positions in the unit cell), enabling the calculation of interatomic distances, bond angles, and octahedral structures. Moreover, this method can be applied not only to X-ray diffraction spectra but also to neutron diffraction spectra.

Currently, many software packages implement the Rietveld method. Among them, *FullProf*<sup>5</sup> is of particular importance. Its advantage is continuous updating in accordance with advances in crystallography and improvements in analysis techniques, which extends its functionality in newer versions.

After analysis of XRD spectra, the unit cell structure of the studied crystals can be reconstructed. In recent years, the *Diamond 3.2* program has become one of the most widely used tools for building crystal structures in 3D format. By inputting symmetry, space group, lattice parameters, and atomic coordinates, it is possible not only to

---

<sup>4</sup> Runčevski, T., Brown, C.M. The Rietveld refinement method: half of a century anniversary // *Crystal Growth & Design*, – 2021. Aug.; v. 21, № 9, – p. 4821-4822.

<sup>5</sup> <https://www.ill.eu/sites/fullprof/>

visualize the crystal structure but also to calculate interatomic distances and bond angles. Furthermore, diffraction patterns corresponding to the given structure can be simulated<sup>6</sup>.

The analysis of Differential Thermal Analysis (DTA) and DSC methods demonstrated that they allow for a sufficiently detailed study of the thermodynamic state of a system. Determining the values of thermodynamic parameters and studying the mechanisms of their variation under external influences enable better characterization of the system. These parameters are important not only for experimental investigations but also for theoretical studies where direct measurement is not possible. The greater the number of experimentally measurable parameters, the more comprehensive the information about the system becomes.

Modern DSC and DTA calorimeters allow the determination of multiple parameters simultaneously. When connected to computers with advanced software, these calorimeters can directly provide several values, although they are still based on mathematical models. In addition, thermal spectra allow the calculation of certain physical parameters. One of the key parameters for understanding temperature-induced processes is the heat capacity, defined as:

$$dQ = C_p dT \quad (3)$$

The specific heat capacity can be expressed as:

$$c_p = \frac{C_p}{m} = \frac{\frac{dQ}{dt}}{m \cdot \frac{dT}{dt}} = \frac{\Phi_S}{m \cdot \beta} = \frac{\Phi_m - \Phi_0}{m \cdot \beta} \quad (4)$$

where  $\Phi$  is the heat flow measured in the DSC spectrum,  $\beta$  is the heating rate,  $m$  is the mass of the sample,  $C_p$  is the heat capacity at constant pressure,  $Q$  is the heat quantity,  $T$  is the absolute temperature, and  $t$  is the time. As seen from equation (4), the specific heat capacity can be easily calculated from experimental results. Since the pressure

---

<sup>6</sup> Pennington, W. DIAMOND - visual crystal structure information system // Journal of Applied Crystallography, – 1999. Aug.; v. 32, № 5, – p. 1028-1029.

in DSC experiments is constant, the specific heat capacity can also be approximated by:

$$c_p = \frac{\Phi}{m \cdot \beta} \quad (5)$$

Knowing the heat capacity makes it possible to calculate, by mathematical means, thermodynamic parameters that cannot be measured directly in the experiment.

The third chapter investigates the influence of cation–cation substitutions on the structure and thermal properties of  $\text{Ge}_{1-x}\text{Ln}_x\text{S}$  chalcogenide semiconductors. Based on the synthesis and X-ray phase analyses of  $\text{Ge}_{1-x}\text{Ln}_x\text{S}$  compounds, it was determined that the maximum optimal concentration of rare-earth elements for obtaining single-phase systems is 1%. This limitation is explained by the ionic radii of the constituent metals. The ionic radius of divalent Ge is  $R_{\text{Ge}^{2+}} = 0.72 \text{ \AA}$ , whereas that of divalent Nd is  $R_{\text{Nd}^{2+}} = 1.17 \text{ \AA}$ . The difference  $\Delta R = 0.45 \text{ \AA}$  is comparable to interatomic distances; therefore, when the Nd content in  $\text{Ge}_{1-x}\text{Nd}_x\text{S}$  exceeds 1%, solid-solution formation ceases and not all Nd atoms can substitute Ge sites.

To elucidate the structural effects induced by cation–cation substitution, the  $\text{Ge}_{0.99}\text{Nd}_{0.01}\text{S}$  compound was synthesized and its crystal structure studied by X-ray diffraction (XRD) at room temperature. For compounds containing rare-earth elements, XRD is the most suitable technique: neutron diffraction is often compromised by the high neutron absorption of heavy rare-earth atoms, while X-rays—scattered by electron clouds—are especially informative for heavier elements. Accordingly,  $\text{Ge}_{0.99}\text{Nd}_{0.01}\text{S}$  was examined with a Bruker D8 ADVANCE diffractometer (Diffrac.Suite),  $\text{CuK}\alpha$  radiation,  $5^\circ < 2\theta < 55^\circ$ , using powdered samples. Diffraction patterns were refined by the Rietveld method in *FullProf*, enabling determination of the crystal system, space group, lattice parameters, atomic coordinates, interatomic distances, and bond angles. The room-temperature XRD pattern of  $\text{Ge}_{0.99}\text{Nd}_{0.01}\text{S}$  is shown in Figure 2.

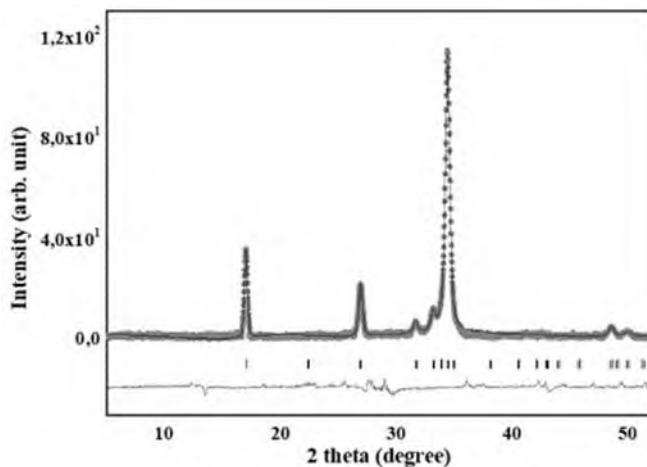


**Figure 2**

(theoretical profile as lines, experimental data as points; vertical ticks denote Miller indices; the horizontal trace shows the difference curve). The refinement established an orthorhombic structure, space group Pnma, with lattice parameters  $a = 4.3165 \text{ \AA}$ ,  $b = 3.6486 \text{ \AA}$  and  $c = 10.4915 \text{ \AA}$ .

Further structural analysis confirmed that  $\text{Ge}_{0.99}\text{Nd}_{0.01}\text{S}$  adopts the same structural type as GeS (Pnma)<sup>7</sup>. The refined atomic coordinates were: Ge and Nd at  $x/a=3/8$ ,  $y/b=1/4$ ,  $z/c=1/6$ ; S at  $x/a=0.1414$ ,  $y/b=1/4$ ,  $z/c=0.1287$ .

The thermal properties of the  $\text{Ge}_{0.99}\text{Nd}_{0.01}\text{S}$  layered crystal were studied comparatively by Differential Scanning Calorimetry (DSC) and Thermogravimetric Analysis (TGA). In DSC, both the heat-flow (black curve) and its differential form (red curve) were recorded over 25–750 °C (see **Figure 3**).

<sup>7</sup> Daşdəmirov, A.O.  $\text{Ge}_{0.99}\text{Nd}_{0.01}\text{S}$  birləşməsinin kristal quruluşu // AJP Fizika, – 2022. Dek.; v. 28, № 4, – s. 7-9.

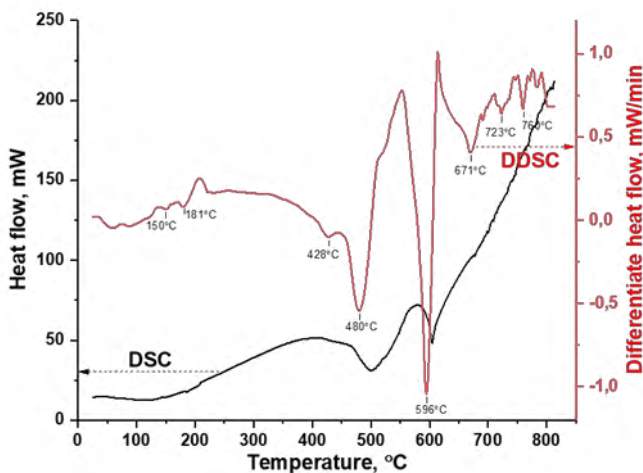


**Figure 3**

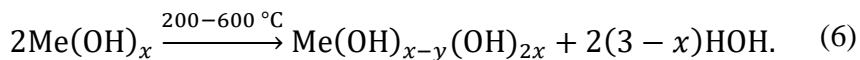
High-resolution data (3654 points) show that the thermal behavior is complex; each feature corresponds to a specific process (evaporation, decomposition, oxidation, melting, phase transition, etc.). While the heat-flow curve splits into two temperature regions, the differential spectrum reveals thermal effects and transitions more clearly; hence both are presented for comparative interpretation<sup>8</sup>.

Within 25–750 °C, thermal effects were observed at 150, 181, 428, 480, 596, 671, 723, and 760 °C. The predominantly endothermic features were attributed to adsorbed H<sub>2</sub>O, CO<sub>2</sub>, and O<sub>2</sub> and their reaction products.

The effects centered at 150 °C and 181 °C are assigned to the decomposition of hydroxyl groups formed by weakly chemisorbed water on the active surface of Ge<sub>0.99</sub>Nd<sub>0.01</sub>S. Such processes typically onset above  $T \geq 100^\circ\text{C}$  and accelerate with temperature until water is

<sup>8</sup> Dashdemirov, A.O., Alekperov, A.S., Aliyev, Y.I. Mechanism and kinetics of thermal processes in Ge<sub>0.99</sub>Nd<sub>0.01</sub>S compound // UNEC Journal of Engineering and Applied Sciences, – 2023. May; v. 3, № 1, – p. 28-32.

fully released. A schematic decomposition mechanism can be written as:



The areas under the DSC peaks correspond to the energy required for each process. The principal four high-temperature effects are highlighted in **Figure 4**, showing different energy expenditures (e.g., integrated energies decreasing from E=186 mC to E=154 mC for peaks centered near 432, 480, 584, 669 °C). Small anomalous features are also visible in the differential heat-flow at  $T > 669^\circ\text{C}$ .

Complementary TGA (and its time derivative) for 25–750 °C is shown in Figure 5. At  $T=25\text{ }^\circ\text{C}$  the sample mass was  $m=16.45\text{ mg}$ , decreasing to  $m=15.74\text{ mg}$  by 494 °C (4.31% loss). A step-like decomposition occurs between 494–601 °C with an additional 38.84% loss. The 601–750 °C region is thermally stable. (Total mass loss  $\approx 43\%$ , accounting for desorption/evaporation, hydroxide breakdown, and phase transition.)

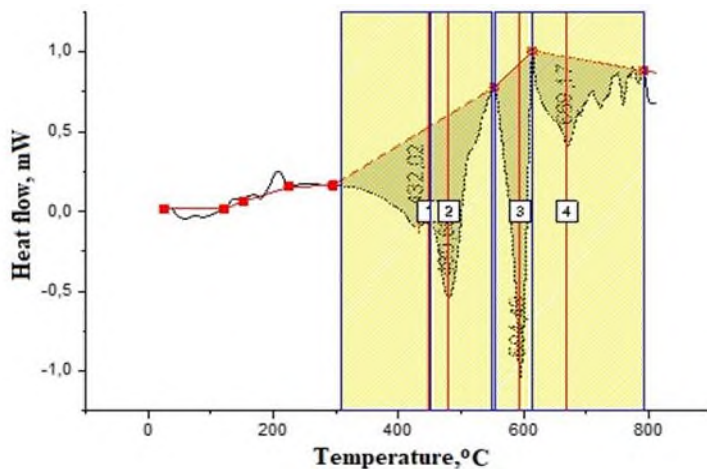


**Figure 4**

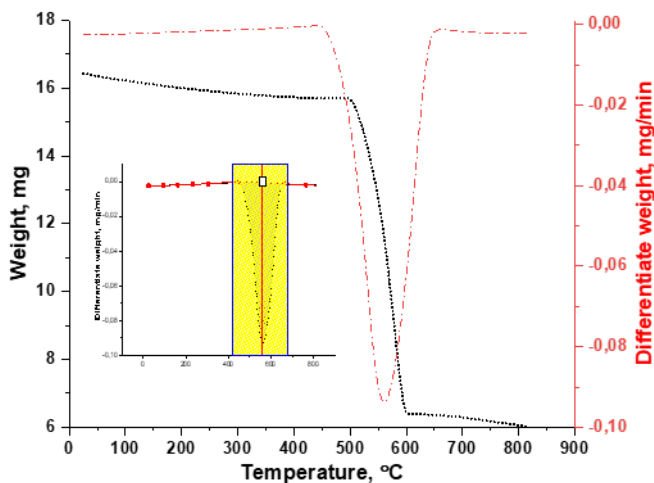


**Figure 5.**

The dominant effect (Figure 4, peak #3) is centered at 596 °C and corresponds to melting (**solid** → **liquid**). As expected, a large energy uptake at melting suppresses the transmitted heat flow (sharp DSC dip), and a concurrent signature is evident in TGA (Figure 5). To visualize this, **Figure 6** plots mass change over 500–650 °C, showing the accelerated mass-loss rate up to completion of melting, followed by a stable liquid-phase region with no further mass decrease upon additional heating.

Overall, the DSC/TGA measurements indicate that  $\text{Ge}_{0.99}\text{Nd}_{0.01}\text{S}$  is thermally robust at elevated temperatures and retains stability beyond its melting point—a desirable attribute for semiconductor devices intended for long-term operation<sup>9</sup>. Similar thermal behavior was observed across  $\text{Ge}_{1-x}\text{Ln}_x\text{S}$  compositions at low substitution levels, suggesting no drastic change in thermodynamic stability for small cation–cation substitutions. For deeper insight, each

<sup>9</sup> Hakhverdiyeva, Z.E. FTIR spectroscopic insights into the bonding structural properties of  $\text{Nd}_{0.5}\text{Ca}_{0.5}\text{MnO}_3$ ,  $\text{Nd}_{0.5}\text{Sr}_{0.5}\text{MnO}_3$ , and  $\text{Pr}_{0.5}\text{Ca}_{0.5}\text{MnO}_3$  / Z.E.Hakhverdiyeva, S.H.Jabarov, E.M.Huseynov [et al.] // Solid State Communications, – 2024. Nov.; v. 391, – p. 115625-1-12

thermoeffect should be analyzed individually in connection with structural aspects.

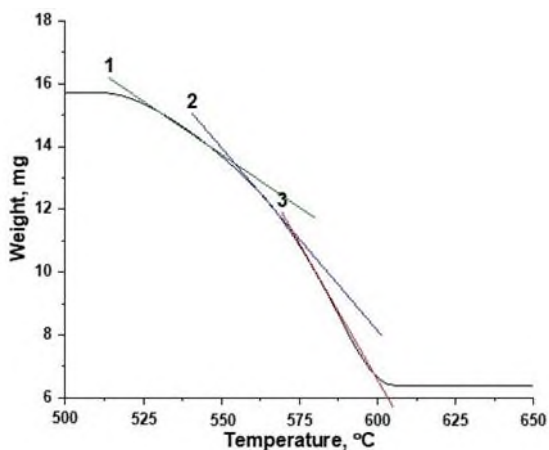


**Figure 6**

Each high-temperature effect reflects an underlying physical-chemical process tied to structural changes, such as defect formation or defect recombination, and ingress/egress of species ( $\text{H}_2\text{O}$ ,  $\text{O}_2$ ,  $\text{CO}_2$ ). In layered  $\text{Ge}_{1-x}\text{Ln}_x\text{S}$ , such species preferentially reside **between layers**, where free volume is larger and interlayer bonding weaker than intralayer bonding, thereby affecting lattice dynamics and thermodynamics.

To probe structural defects, germanium monosulfide thin films were prepared on glass by thermal evaporation under high vacuum ( $10^{-9}$  Torr) with thicknesses  $d = 250, 500, 750$  nm and investigated via **Doppler Broadening Annihilation Spectroscopy (DBAS)** over 0–18 keV positron energy. Experimental datasets were calibrated using the **VEPFIT** code, and **Electron Momentum Distribution (EMD)**

spectra were computed. Peak intensities in EMD were assigned via superposition of positron–electron wavefunctions<sup>10</sup>.

In positron spectroscopy, the S parameter corresponds to annihilation with low-momentum valence electrons (increases with defect concentration), while W corresponds to high-momentum core electrons (increases with defect reduction). Depth profiles of S(E) and W(E) for GeS films (**Figure 7**) indicate that S is highest at E = 1.5 keV due to surface annihilation and surface effects, then decreases<sup>11</sup> approximately exponentially as energy (and mean depth) increase.

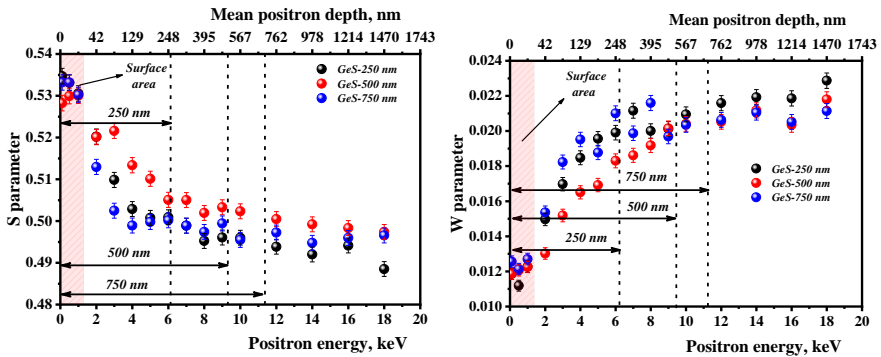


**Figure 7**

Using

$$Z = A/\rho \times E^n$$

with  $A=40$ ,  $n=1.6$ ,  $E$  in keV and density  $\rho$ , the mean implantation depth  $Z$  (nm) was obtained; at 18 keV the penetration depth is

<sup>10</sup> Son, L.Th. Positron annihilation study of lattice defects and nanoporous structures in  $Mn^{4+}$  doped  $K_2SiF_6$  nanophosphors exhibiting high quantum yield / L.Th.Son, T.Th.Doan, P.T.Phuc [et al.] // Radiation Physics and Chemistry, – 2022. Jun.; v. 195, – p. 110064-1-9.

<sup>11</sup> Samadov, S. Study of germanium sulfide thin films by doppler broadening spectroscopy / S.Samadov, A.Sidorin, A.Dashdemirov [et al.] // Indian Journal of Physics, – 2025. Jul.; – pp. 1-6.

$\sim 1.47 \mu\text{m}$ . Positrons with  $E \sim 0\text{-}1.5 \text{ keV}$  probe the surface, whereas  $E > 6, 9, 12 \text{ keV}$  probe the substrate interior for  $d = 250, 500, 750 \text{ nm}$ , respectively; intermediate energies emphasize the film/substrate interface.

Comparing films at identical positron energies shows that the defect concentration is maximal for  $d = 500 \text{ nm}$ , which is attributed to the completion of phase formation in the thicker  $d = 750 \text{ nm}$  films. From S–W correlations (Figure 8), the predominant defects are identified as vacancies<sup>12</sup>. Partial surface oxidation was detected, decreasing with depth.

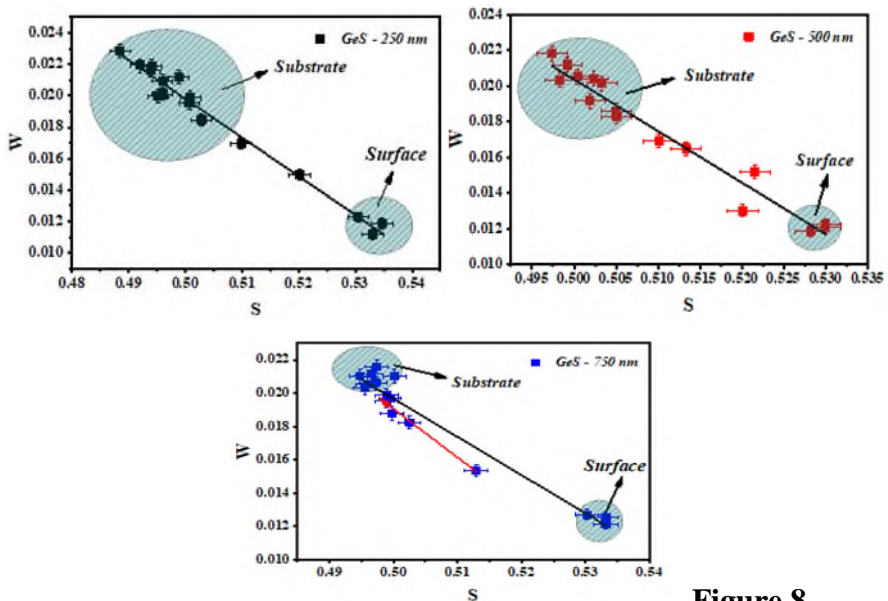


**Figure 8**

At the end of the chapter, the obtained results were analyzed and substantiated by comparing them with those reported in previous studies. It was shown that:

<sup>12</sup> Huomo, H. Positron diffusion in Mo: The role of epithermal positrons / H.Huomo, A.Vehanen, M.D.Bentzon [et al.] // Physical Review B, – 1987. May; v. 35, № 15, – p. 8252-8255.

As a result of the synthesis and X-ray phase analysis of  $\text{Ge}_{1-x}\text{Ln}_x\text{S}$  compounds, it was determined that the optimal concentration of rare-earth elements required to obtain single-phase systems is at most 1%. This process is explained by the ionic radii of the constituent metals. The ionic radius of Ge in the divalent state is  $R_{\text{Ge}^{2+}} = 0.72 \text{ \AA}$ , while that of Nd in the divalent state is  $R_{\text{Nd}^{2+}} = 1.17 \text{ \AA}$ . The difference in ionic radii is  $\Delta R = 0.45 \text{ \AA}$ , which is comparable to interatomic distances. Therefore, if the Nd concentration in the  $\text{Ge}_{1-x}\text{Nd}_x\text{S}$  system exceeds 1%, dissolution does not occur, and Nd atoms cannot fully substitute Ge atoms. As a result, they are chaotically distributed between the layers. The main reason is that the NdS crystal does not possess the same structure as GeS. Structural studies showed that NdS crystallizes in the cubic Fm-3m space group with high symmetry. Hence, Nd atoms cannot easily replace Ge atoms in the GeS compound. For this reason, the maximum concentration of rare-earth elements in  $\text{Ge}_{1-x}\text{Ln}_x\text{S}$  compounds for obtaining single-phase systems should not exceed 1%.

Structural studies carried out by the X-ray diffraction method and analyzed using the Rietveld method in the Mag2Pol program established that the crystal structure of the  $\text{Ge}_{0.99}\text{Nd}_{0.01}\text{S}$  compound corresponds to the orthorhombic Pnma space group. The unit cell parameters were determined as:  $a = 4.3165 \text{ \AA}$ ,  $b = 3.6486 \text{ \AA}$ , and  $c = 10.4915 \text{ \AA}$ . The atomic coordinates of Ge and Nd were  $x/a = 3/8$ ,  $y/b = 1/4$ ,  $z/c = 1/6$ , while the coordinates of sulfur atoms were  $x/a = 0.1414$ ,  $y/b = 1/4$ ,  $z/c = 0.1287$ . It was confirmed that the crystal structure of  $\text{Ge}_{0.99}\text{Nd}_{0.01}\text{S}$  is consistent with that of GeS. Minor differences in the crystallographic parameters were explained by the difference in ionic radii.

The thermal properties of the  $\text{Ge}_{0.99}\text{Nd}_{0.01}\text{S}$  layered crystal were comparatively studied by Differential Scanning Calorimetry (DSC) and Thermogravimetric Analysis (TGA). In the temperature range  $25 \text{ }^\circ\text{C} \leq T \leq 750 \text{ }^\circ\text{C}$ , thermal effects were observed at  $T = 150 \text{ }^\circ\text{C}$ ,  $181 \text{ }^\circ\text{C}$ ,  $428 \text{ }^\circ\text{C}$ ,  $480 \text{ }^\circ\text{C}$ ,  $596 \text{ }^\circ\text{C}$ ,  $671 \text{ }^\circ\text{C}$ ,  $723 \text{ }^\circ\text{C}$ , and  $760 \text{ }^\circ\text{C}$ . These effects, primarily accompanied by energy absorption, were explained by the presence of water, carbon, and oxygen gases absorbed into the samples

and their resulting compounds. It was established that in  $\text{Ge}_{0.09}\text{Nd}_{0.01}\text{S}$ , a phase transition occurs at  $T = 596\text{ }^\circ\text{C}$ , during which the system passes from the solid to the liquid state. The structural aspects of each thermal transition were analyzed, showing that the energy absorbed during decomposition and evaporation processes was also expended on the recombination of defects formed in the structure. It was determined that effects occurring at approximately  $T \sim 100\text{ }^\circ\text{C}$  are related to the evaporation of water molecules trapped in the samples. Such processes require little heat energy. However, if water molecules bond with metal atoms in the compounds to form hydroxide groups, then sufficient thermal energy is required for the compound's decomposition, water evaporation, and the recombination of defects generated during this process.

Phase formation and defect states in germanium monosulfide thin films were investigated. Based on positron annihilation spectra, the energy dependences of the S and W parameters and the W(S) dependence were obtained. From these dependencies, it was determined that the defects formed in the thin films are mainly of vacancy type. Partial oxidation was detected on the surface of the thin films, and it was observed that oxygen bonds decrease with increasing depth from the surface.

In the **fourth chapter** investigates how cation–cation substitutions affect the optical properties of  $\text{Ge}_{1-x}\text{Ln}_x\text{S}$  ( $\text{Ln} = \text{Gd}, \text{Sm}, \text{Nd}$ ) chalcogenide semiconductors. From the study of undoped GeS and lightly doped layered single crystals  $\text{Ge}_{1-x}\text{Ln}_x\text{S}$  (with small concentrations of Nd, Sm, and Gd), it was found that differences in ionic radii and electronic configurations of the substituting cations significantly influence the optical response. As is well known, both structural parameters and electronic processes in semiconductors vary with temperature. In GeS crystals containing Nd and Sm, the maxima of the photoconductivity spectra shift toward longer wavelengths as temperature increases, indicating a decrease in photosensitivity. In the

case of Ge  $\rightarrow$  Nd substitution, pronounced changes occur in the photoconductivity of GeS: an additional maximum appears at photon energy  $E=1.4\text{eV}$  within  $200\text{ K} < T < 250\text{ K}$  (Figure 9). This is attributed to the dissociation of exciton–impurity complexes under thermal stimulation.

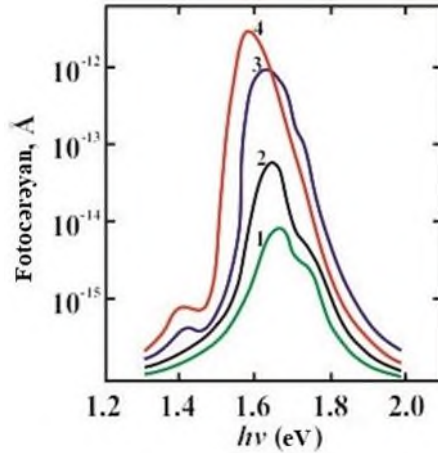


**Figure 9.** Photoconductivity spectrum of the  $\text{Ge}_{0.99}\text{Nd}_{0.01}\text{S}$  layered crystal: 1 –  $T=80\text{K}$ ; 2 –  $T=200\text{K}$ ; 3 –  $T=300\text{K}$ ; 4 –  $T=320\text{K}$ .

A similar effect is observed for Ge  $\rightarrow$  Sm substitution: in the same temperature range, an additional maximum appears at  $E=1.3\text{eV}$ , likewise explained by the dissociation of exciton–impurity complexes.

In contrast to Nd and Sm, Gd behaves differently. It was established that Gd atoms do not form complex atomic aggregates within the GeS matrix, a behavior ascribed to the stable electronic configuration of gadolinium, which disfavors complex formation. This distinction manifests in the optical properties of  $\text{Ge}_{1-x}\text{Gd}_x\text{S}$  layered single crystals. For assessing application potential, it is essential to probe the response

of materials under external stimuli, notably ionizing radiation. In spaceborne devices, accelerators, and nuclear technologies, radiation doses can be substantial, potentially degrading device functionality. It was found that GeS crystals subjected to rare-earth cation–cation substitutions retain optical activity even under ionizing radiation. However, low-dose (**D=30krad**) gamma irradiation does not induce additional maxima in the photoconductivity spectra of  $\text{Ge}_{1-x}\text{Ln}_x\text{S}$  layered single crystals at low temperatures. (figure10, 11).

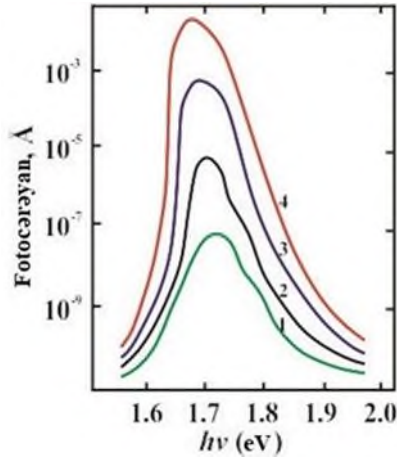


**Figure 10.** Low-temperature photoconductivity spectra of  $\text{Ge}_{0.995}\text{Nd}_{0.005}\text{S}$  irradiated with gamma quanta at  $D=30\text{D}=30\text{D}=30\text{ krad}$ : 1)  $T=80\text{T}=80\text{T}=80\text{ K}$ ; 2)  $T=200\text{T}=200\text{T}=200\text{ K}$ ; 3)  $T=300\text{T}=300\text{T}=300\text{ K}$ ; 4)  $T=320\text{T}=320\text{T}=320\text{ K}$ .

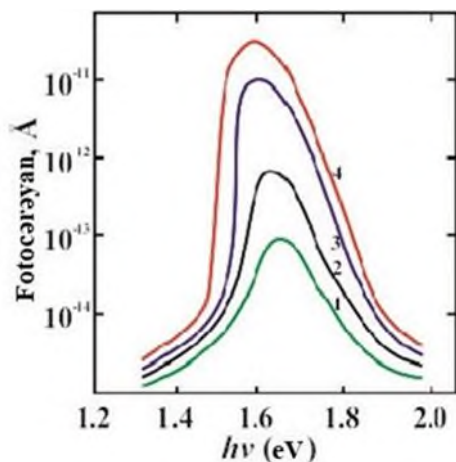


**Figure 11.** Low-temperature photoconductivity spectra of  $\text{Ge}_{0.99}\text{Nd}_{0.01}\text{S}$  irradiated with gamma quanta at  $D=30D=30D=30$  krad: 1)  $T=80T=80T=80$  K; 2)  $T=200T=200T=200$  K; 3)  $T=300T=300T=300$  K; 4)  $T=320T=320T=320$  K.

This behavior is explained by the absence of exciton–impurity complex formation due to the high structural order maintained in the irradiated crystals.

The chapter concludes with a detailed discussion of the above findings.

In **chapter five**, the effect of cation–cation substitutions on the structure and thermal properties of  $\text{Cu}_{2-x}\text{Tm}_x\text{Se}$  chalcogenide semiconductors was investigated. The study examined the structure of the  $\text{Cu}_2\text{Se}$  compound and its structural phase transitions, as well as the structural modifications and thermal characteristics arising from partial  $\text{Cu} \rightarrow \text{Tm}$  substitutions.

Analysis of the spectra obtained in the temperature range  $T = 290\text{--}1000$  K for  $\text{Cu}_2\text{Se}$  revealed a structural phase transition. It was determined that, under ambient conditions, this compound exhibits an orthorhombic crystal structure (Figure 12). As seen in the figure,  $\text{Cu}_2\text{Se}$  possesses a relatively simple structure: copper atoms occupy

the lattice nodes of the orthorhombic unit cell, while selenium chalcogen atoms, positioned around the central copper atom, form an octahedron through covalent bonding, thus constituting the elementary cell. At temperatures  $T \geq 423$  K, the diffraction lines characteristic of  $\text{Cu}_2\text{Se}$  at room temperature disappear, and new diffraction lines corresponding to a different phase emerge within the same angular range.

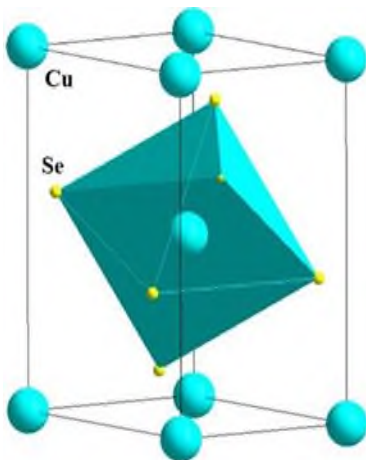


**Figure 12.** Orthorhombic crystal structure of  $\text{Cu}_2\text{Se}$  at room temperature

Analysis of the X-ray diffraction spectra revealed that at  $T = 423$  K, the number of diffraction maxima sharply decreases. This phenomenon was attributed to a phase transformation. Three new maxima were identified in the diffraction pattern, corresponding to the Miller indices (111), (222), and (333). It was established that this phase corresponds to a cubic crystal structure. The three-dimensional crystal structure of  $\text{Cu}_2\text{Se}$  in this cubic phase at  $T = 423$  K is presented in Figure 13.

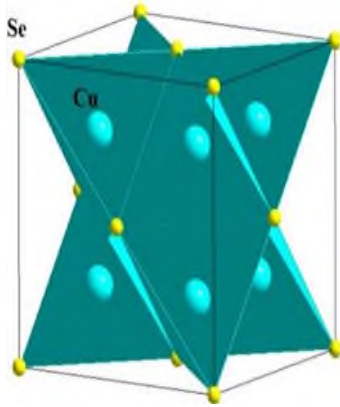


**Figure 13.** Cubic crystal structure of  $\text{Cu}_2\text{Se}$  at  $T = 423 \text{ K}$

The orthorhombic-to-cubic phase transition occurs at  $T = 405 \text{ K}$ , resulting in the formation of a highly symmetric phase. The crystallographic parameters for each phase were determined and are summarized in Table 1.

**Table 1.** Crystallographic parameters of  $\text{Cu}_2\text{Se}$  at elevated

| $T, \text{ K}$ | Sinqoniya  | Özək parametrləri, Å |         |          | Fəza qrupu        |
|----------------|------------|----------------------|---------|----------|-------------------|
|                |            | $a$                  | $b$     | $c$      |                   |
| 293            | Ortorombik | 4.11713              | 7.03224 | 20.34708 | P222 <sub>1</sub> |
| 323            |            | 4.11812              | 7.03415 | 20.35119 |                   |
| 373            |            | 4.12176              | 7.03851 | 20.36772 |                   |
| 405            |            | 4.12518              | 7.04232 | 20.38031 |                   |
| 423            | Kubik      | 5.83909              | -       | -        | F-43m             |
| 473            |            | 5.84425              | -       | -        |                   |
| 523            |            | 5.85566              | -       | -        |                   |
| 573            |            | 5.86214              | -       | -        |                   |

From the lattice parameter values, it is evident that increasing temperature leads to an expansion of the unit cell. This expansion differs depending on both the phase and the specific parameter. In the

orthorhombic phase within  $T = 293\text{--}405$  K, the variations are  $\Delta a = 0.00805$  Å,  $\Delta b = 0.01008$  Å, and  $\Delta c = 0.03323$  Å. The nonuniform changes in these parameters indicate a change in symmetry, resulting in a phase transition. In the cubic phase, within  $T = 423\text{--}573$  K, the parameter changes were  $\Delta a = \Delta b = \Delta c = 0.02305$  Å. Based on the temperature dependence of the lattice parameters in the orthorhombic and tetragonal phases, the coefficients of thermal expansion along different crystallographic directions were calculated. Anisotropy of the linear thermal expansion coefficients was observed in the [100], [010], and [001] directions of the low-temperature orthorhombic phase.

The influence of  $\text{Cu} \rightarrow \text{Tm}$  substitutions on the crystal structure of  $\text{Cu}_2\text{Se}$  was also studied. For this purpose, compounds of the  $\text{Cu}_{2-x}\text{Tm}_x\text{Se}$  ( $x = 0.1, 0.2, 0.3$ ) system were synthesized using the conventional high-vacuum methods characteristic of chalcogenide semiconductors, and their structural features were examined. X-ray diffraction studies at room temperature revealed that the crystal structure of these compounds significantly differs from that of pure  $\text{Cu}_2\text{Se}$  and corresponds instead to a rhombohedral symmetry with space group  $R\text{-}3m(166)$ . For each composition with varying Tm concentrations, lattice parameters and atomic coordinates were determined. The differences in crystallographic parameters among  $\text{Cu}_{1.9}\text{Tm}_{0.1}\text{Se}$ ,  $\text{Cu}_{1.7}\text{Tm}_{0.3}\text{Se}$ , and  $\text{Cu}_{1.5}\text{Tm}_{0.5}\text{Se}$  were attributed to the disparity between the ionic radii of Cu and Tm atoms.

The thermal properties of the  $\text{Cu}_{2-x}\text{Tm}_x\text{Se}$  system were investigated by Differential Scanning Calorimetry (DSC) and Thermogravimetric Analysis (TGA) within the temperature range  $T = 30\text{--}800$  °C. It was established that increasing the concentration of Tm atoms reduces the melting temperature of the compounds. Melting points were determined for the  $\text{Cu}_{2-x}\text{Tm}_x\text{Se}$  system, and the mechanisms of temperature-induced changes at high temperatures were clarified. During the solid–liquid phase transition, mass loss was observed, and the magnitude of this loss was determined as a function of Tm concentration. At the end of the chapter, the obtained results were summarized, the structural aspects of the thermal properties were

analyzed, and the influence of cation–cation substitutions on thermal behavior was discussed.

In chapter six, the influence of cation–cation substitutions on the optical properties of  $\text{Cu}_{2-x}\text{Tm}_x\text{Se}$  chalcogenide semiconductors was investigated. To examine the effect of partial replacement of Cu atoms with rare-earth elements on the formation of optical properties,  $\text{Cu}_{2-x}\text{Tm}_x\text{Se}$  ( $x = 0.1, 0.2, 0.3$ ) compounds were synthesized, and their optical characteristics were studied. Under ambient conditions, the optical absorption spectra of  $\text{Cu}_{1.9}\text{Tm}_{0.1}\text{Se}$ ,  $\text{Cu}_{1.8}\text{Tm}_{0.2}\text{Se}$ , and  $\text{Cu}_{1.7}\text{Tm}_{0.3}\text{Se}$  were obtained (Figure 14).

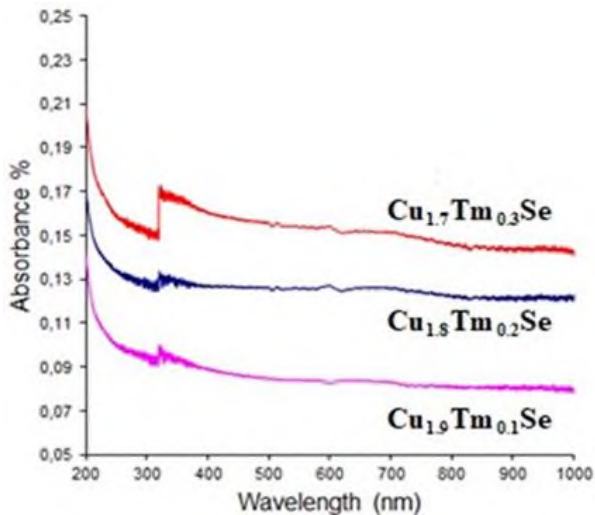


**Figure 14**

Analysis of these spectra allowed for the experimental determination of the band gap. It was found that the band gap for  $\text{Cu}_{1.9}\text{Tm}_{0.1}\text{Se}$  is  $E_g = 1.25$  eV. With increasing Tm concentration, the band gap widens:  $\text{Cu}_{1.8}\text{Tm}_{0.2}\text{Se}$  exhibited  $E_g = 1.35$  eV, while  $\text{Cu}_{1.7}\text{Tm}_{0.3}\text{Se}$  showed  $E_g = 1.44$  eV. These results indicate that with increasing Tm concentration, the semiconducting behavior is enhanced due to differences in ionic radii and, more importantly, electronic configurations of Tm and Cu atoms.

Structural phase analysis using X-ray diffraction confirmed that all compositions are single-phase systems, in which the substituted Tm atoms fully replace Cu atoms at low concentrations. The ionic radius of Cu is  $R_{\text{Cu}} = 0.96 \text{ \AA}$ , while that of Tm is  $R_{\text{Tm}} = 1.36 \text{ \AA}$ , resulting in a significant difference of  $\Delta R = 0.4 \text{ \AA}$  (approximately 40% larger than Cu). Such a large substitution induces lattice expansion, which leads to partial separation of electronic bands in the energy structure. While this expansion does not strongly manifest in lattice parameters, it significantly affects electronic processes, explaining the observed increase in band gap with Tm concentration. Experimental measurements revealed that the difference in band gap between  $\text{Cu}_{1.9}\text{Tm}_{0.1}\text{Se}$  and  $\text{Cu}_{1.7}\text{Tm}_{0.3}\text{Se}$  is approximately  $\Delta E_g \approx 0.2 \text{ eV}$ .

It is known that Cu atoms generally enter the  $\text{Cu}_2\text{Se}$  lattice in a monovalent state, whereas rare-earth elements such as Tm are predominantly trivalent, though valence fluctuations can occur in some compounds. In the case of  $\text{Cu}_{2-x}\text{Tm}_x\text{Se}$ , Tm atoms enter the lattice in a monovalent state, which is feasible only at low concentrations. At higher concentrations, full substitution is not possible, and Tm atoms act as dopants distributed throughout the lattice.

To further explore the optical properties, photoluminescence spectra were obtained (Figure 15). For  $\text{Cu}_{1.9}\text{Tm}_{0.1}\text{Se}$ , two maxima were observed at  $\lambda = 416 \text{ nm}$  and  $\lambda = 433 \text{ nm}$ . The spectra for  $\text{Cu}_{1.8}\text{Tm}_{0.2}\text{Se}$  were nearly identical, with similar peak positions and intensities. However, for  $\text{Cu}_{1.7}\text{Tm}_{0.3}\text{Se}$ , two maxima at  $\lambda = 416 \text{ nm}$  and  $\lambda = 436 \text{ nm}$  were observed, with significantly higher intensities compared to those of  $\text{Cu}_{1.9}\text{Tm}_{0.1}\text{Se}$  and  $\text{Cu}_{1.8}\text{Tm}_{0.2}\text{Se}$ . This indicates that increasing Tm concentration enhances the density of optically active centers, thereby increasing photoluminescence intensity.

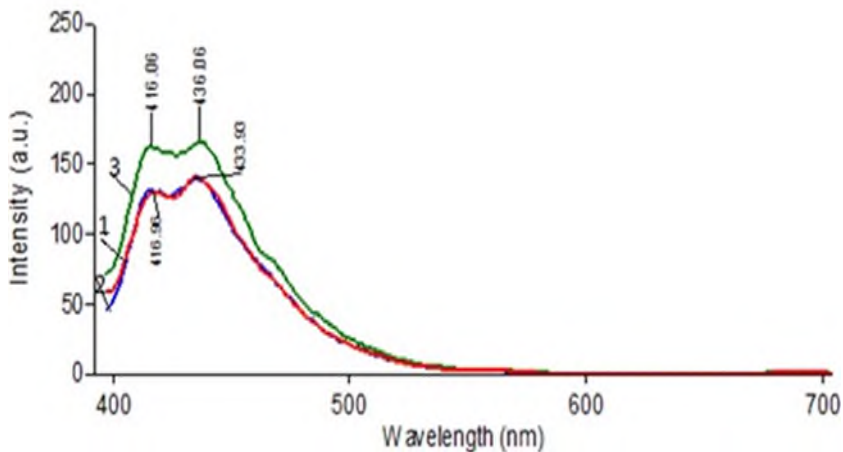


**Figure 15**

To provide a comparative analysis, excitation and emission spectra were also obtained (Figure 16).

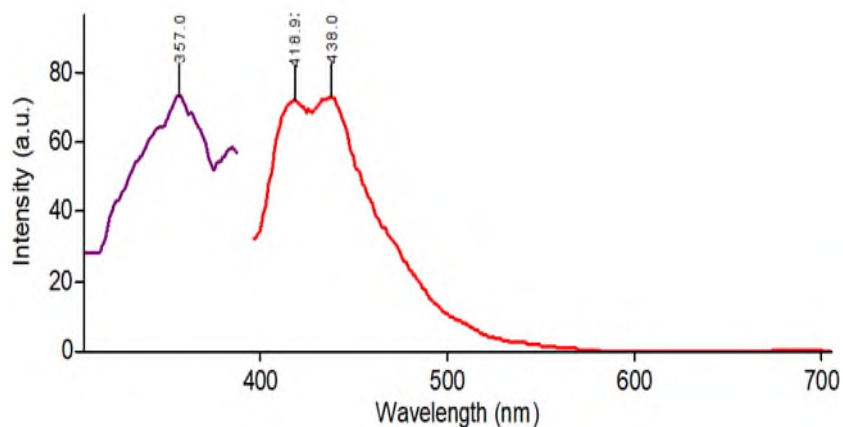


**Figure 16**

Computational analysis using **Quantum Wise – Atomistix Tool Kit** confirmed that the band structure of pure  $\text{Cu}_2\text{Se}$  is metallic, with

overlapping bands and a zero band gap ( $E_g = 0$  eV). The density of states (DOS) and electronic band calculations revealed a complex electronic structure consistent with metallic behavior. However, experimental investigations showed that partial substitution of Cu by Tm induces semiconducting behavior in  $\text{Cu}_{2-x}\text{Tm}_x\text{Se}$  compounds, even at low substitution levels ( $x = 0.1, 0.2, 0.3$ ), with measurable band gaps ranging from  $E_g = 1.25$  eV to  $E_g = 1.44$  eV. These findings confirm that rare-earth cation substitutions significantly influence the electronic and optical properties of chalcogenides.

At the end of the chapter, the results were analyzed and explained.

## CONCLUSIONS

Based on the comprehensive experimental studies of GeS and  $\text{Cu}_2\text{Se}$  compounds partially substituted with rare-earth metals, the following conclusions were drawn:

1. Structural studies of GeS crystals with partial substitution of Ge by Nd, Sm, and Gd showed that up to 1% substitution yields single-phase compounds with an orthorhombic Pnma crystal structure.
2. Thermal studies of  $\text{Ge}_{0.99}\text{Nd}_{0.01}\text{S}$  in the range  $25\text{ }^\circ\text{C} \leq T \leq 750\text{ }^\circ\text{C}$  revealed thermal effects at  $T = 150\text{ }^\circ\text{C}$ ,  $181\text{ }^\circ\text{C}$ ,  $428\text{ }^\circ\text{C}$ ,  $480\text{ }^\circ\text{C}$ ,  $596\text{ }^\circ\text{C}$ ,  $671\text{ }^\circ\text{C}$ ,  $723\text{ }^\circ\text{C}$ , and  $760\text{ }^\circ\text{C}$ , corresponding to processes such as decomposition, evaporation, and defect recombination.
3. A phase transition was observed in  $\text{Ge}_{0.99}\text{Nd}_{0.01}\text{S}$  at  $T = 596\text{ }^\circ\text{C}$ , corresponding to melting (solid–liquid transition).
4. Optical conductivity studies of Nd-substituted GeS revealed red-shifts in spectral maxima with increasing temperature, indicating reduced photosensitivity. An additional maximum at  $E = 1.4$  eV (200–250 K) was attributed to exciton–impurity complex dissociation.
5. Photoluminescence spectra of GeS and  $\text{Ge}_{0.99}\text{Gd}_{0.01}\text{S}$  showed a maximum at  $\lambda = 685$  nm, with significantly higher intensity for

the Gd-substituted sample, attributed to the  $6P_j \rightarrow 8S_j$  transition of  $Gd^{3+}$  (4f-4f transition).

6. Structural analysis showed that  $Cu_{2-x}Tm_xSe$  ( $x = 0.1, 0.2, 0.3$ ) compounds crystallize in the rhombohedral system with space group R-3m(166). Lattice parameters increase with Tm concentration due to the difference in ionic radii between Cu and Tm.
7. Thermal studies of  $Cu_{1.9}Tm_{0.1}Se$ ,  $Cu_{1.7}Tm_{0.3}Se$ , and  $Cu_{1.5}Tm_{0.5}Se$  revealed thermal effects at  $T = 140$  °C, attributed to decomposition of hydroxide groups formed by adsorbed water molecules with Cu and Tm atoms.
8. Thermal analysis of  $Cu_{2-x}Tm_xSe$  showed endothermic effects above  $T > 600$  °C associated with melting, with the melting point decreasing as Tm concentration increased.
9. Absorption spectra of  $Cu_{2-x}Tm_xSe$  revealed optical activity dependent on Tm concentration, with a peak at  $\lambda = 320$  nm attributed to the f-f transition ( ${}^3H_6 \rightarrow {}^1D_2$ ) of  $Tm^{3+}$  ions.
10. The band gaps of  $Cu_{1.9}Tm_{0.1}Se$ ,  $Cu_{1.8}Tm_{0.2}Se$ , and  $Cu_{1.7}Tm_{0.3}Se$  were determined as  $E_g = 1.25$  eV, 1.35 eV, and 1.44 eV, respectively. The results confirm that increasing Tm concentration systematically increases the band gap.

### **The list of published scientific works on the topic of the dissertation:**

1. Гасанов, О.М. Влияние атомов Gd на фоточувствительность монокристалла SnS / О.М.Гасанов, Х.А.Адгезалова, А.О.Дашдемиров [и др.] // Журнал «Прикладная физика», – Москва: – 2017. Апр.; № 4, – с. 42-45
2. Мадатов, Р.С. Эффект электрического переключения проводимости с памятью в структуре Ag-GeS:Nd-Ag / Р.С.Мадатов, А.С.Алекперов, А.О.Дашдемиров [и др.] // Журнал «Прикладная физика», – Москва: – 2017. Дек.; № 6, – с. 90-94.
3. Ismailov, Sh.S. Pr  $xSn_{1-x}Se$  sistem ərintilərinin elektrofiziki xassələrinə  $\gamma$ -şüalarının və termoemanın təsiri / Sh.S.Ismailov, J.I.Huseynov, A.O.Daşdəmirov [et al.] // Journal of Radiation

- Researches, – 2018. May; v. 5, № 2, – p. 77-81
4. Гасанов, О.М., Адгезалова, Х.А., Гусейнов, Дж.И., Дашдемиров, А.О. Фотоэлектрические свойства монокристалла  $(\text{SnS})_{0.999}(\text{SmS})_{0.001}$  // XXV Международная научно-техническая конференция и школа по фотоэлектронике и приборам ночного видения, – Москва: – 24-26 мая, – 2018, – с. 581-582
  5. Aliyev, Y.I., Asadov, Y.G., Dashdemirov, A.O. X-ray study of the crystal structure of  $\text{Cu}_{1.75}\text{Te}$  // LIII Школа ПИЯФ по физике конденсированного состояния ФКС-2019, – Санкт-Петербург: – 11 – 16 марта, – 2019, – с. 43
  6. Алекперов, А.С. Получение гетероперехода Ge–GeS : Nd и исследование спектральной характеристики / А.С.Алекперов, А.О.Дашдемиров, Н.А.Исмайылова [и др.] // Физика и техника полупроводников, – 2020. Июнь; т. 54, № 11, – с. 1193-1196
  7. Alakbarov, A.S. Effect of the gamma irradiation on the structure and exciton photoconductivity of layered GeS:Sm single crystal / A.S.Alakbarov, A.O.Dashdemirov, R.B.Bayramli [et al.] // Advanced Physical Research, – 2021. Apr.; v. 3, № 1, – p. 39-45
  8. Алекперов, А.С. Влияние гамма-облучения на эффект термопереключения монокристалла GeS: Nd / А.С.Алекперов, А.О.Дашдемиров, Т.Г.Нагиев [и др.] // Физика и техника полупроводников, – 2021. Июнь; т. 55, № 7, – 537-540
  9. Dashdemirov, A.O. Electronic and optical properties of GeS and GeS: Gd / A.O.Dashdemirov, S.G.Asadullayeva, A.S.Alekperov [et al.] // International Journal of Modern Physics B, – 2021. Aug.; v. 35, № 30, – p. 2150305-1-12.
  10. Aliyev, Y.İ., Dashdemirov, A.O. Thermodynamic parameters of  $\text{AgCu}_{1-x}\text{Fe}_x\text{S}$  compounds under non-isothermal conditions // 10<sup>th</sup> Rostocker International Conference: “Thermophysical Properties for Technical Thermodynamics”, – Rostock, Germany: – 09 – 10 September, 2021, – p.78.
  11. Alekperov, A.S. High-Temperature Exciton Photoconductivity of  $\text{Ge}_{1-x}\text{Nd}_x\text{S}$  Crystals / A.S.Alekperov, A.O.Dashdemirov, A.E.Shumskaya [et al.] // Crystallography, – 2021. Dec.; v. 66, № 7, – p.

1320-1325.

12. Alekperov, A.S., Dashdemirov, A.O., Asadullayeva, S.G., Jabarov, S.H., Qafarova, G.A. Photoluminescence Properties of GeS: Nd Layered Crystals in Room Temperature // 7<sup>th</sup> International Conference MTR-2021: Modern Trends in Physics, – Baku: BSU, – 15-17 December, – 2021, – p. 189-191.
13. Alekperov, A.S., Dashdemirov, A.O. Photoconductivity of Ge<sub>1-x</sub>Nd<sub>x</sub>S at High Temperatures // International Conference: Condensed Matter Research at the IBR-2, – Dubna: – 25-29 April, – 2022, – p. 180.
14. Aliyev, Y.I. Vibrational properties of YbAs<sub>2</sub>S<sub>4</sub> and YbAs<sub>2</sub>Se<sub>4</sub> compounds: by infrared spectroscopy / Y.I.Aliyev, F.G.Asadov, T.M.Ilyasli [et al.] // Ferroelectrics, – 2022. Dec.; v. 599, № 1, – p. 78-82.
15. Aliyev, Y.I. Vibrational properties of YbAs<sub>2</sub>S<sub>4</sub> and YbAs<sub>2</sub>Se<sub>4</sub> compounds: by infrared spectroscopy / Y.I.Aliyev, F.G.Asadov, T.M.Ilyasli [et al.] // Ferroelectrics, – 2022. Dec.; v. 599, № 1, – p. 78-82.
16. Daşdemirov, A.O. Ge<sub>0.99</sub>Nd<sub>0.01</sub>S birləşməsinin kristal quruluşu // AJP Fizika, – 2022. Dek.; v. 28, № 4, – s. 7-9.
17. Niftiyev, N.N. Optical properties of FeGaInS<sub>4</sub> single crystals under laser excitation / N.N.Niftiyev, A.O.Dashdemirov, F.M.Mammadov [et al.] // Journal of Applied Spectroscopy, – 2023. Jan.; v. 89, № 6, – p. 1147-1149.
18. Мурадов, М.Б. Диэлектрические свойства слоистых монокристаллов MnGaInSe<sub>4</sub> в переменном электрическом поле / М.Б.Мурадов, Н.Н.Нифтиев, А.О.Дашдемиров [и др.] // Электронная обработка материалов, – 2023. Фев.; т. 59, № 2, – с. 61-66..
19. Asadullayeva, S.G. Infrared luminescence of GeS: Nd layered crystals / S.G.Asadullayeva, A.O.Dashdemirov, A.S.Alekperov [et al.] // Advanced Physical Research, – 2023. Apr.; v. 5, № 1, – p. 12-18.
20. Dashdemirov, A.O., Alekperov, A.S., Aliyev, Y.I. Mechanism and kinetics of thermal processes in Ge<sub>0.99</sub>Nd<sub>0.01</sub>S compound //

- UNEC Journal of Engineering and Applied Sciences, – 2023. May; v. 3, № 1, – p. 28-32.
21. Niftiyev, N.N. Dielectric properties of layered MnGaInSe<sub>4</sub> single crystals in an alternating electric field / N.N.Niftiyev, A.O.Dashdemirov, F.M.Mamedov [et al.] // Surface engineering and applied electrochemistry, – 2023. Oct.; v. 59, № 5, – p. 644-648.
  22. Дашдемиров, А.О. Структурный фазовый переход в Cu<sub>2</sub>Se при высокой температуре // Международная конференция «Фазовые переходы, критические и нелинейные явления в конденсированных средах», – Махачкала: – 10 – 15 сентября, – 2023, – с. 124-125.
  23. Daşdəmirov, A.O., Ələkbərov, A.S. Nadir torpaq metallarının GeSe laylı monokristalının fotoelektrik və optik xassələrinə təsiri // Azerbaijan Journal of Physics, – 2023. Nov.; – p. 11-13.
  24. Dashdemirov, A.O. Structural aspects of the thermal properties of the Cu<sub>2</sub>Se / A.O.Dashdemirov, Y.I.Aliyev, R.J.Bashirov [et al.] // International Journal of Modern Physics B, – 2024. Apr.; v. 38, № 10, – p. 2450150-1-15.
  25. Daşdəmirov, A.O., Əkərbərov, A.S. GeS laylı monokristalından alternativ enerji mənbəyi kimi istifadə olunma perspektivləri // «İnnovativ ekosistemlərin inkişafında universitetlərin rolu», – Gəncə: ATU, – 5 – 6 noyabr, – 2024, – s. 127-129.
  26. Ələkbərov, A.S., Daşdəmirov, A.O. GeSe:Nd laylı monokristalında eksiton effekti // «Fizika və Astronomiya problemləri» XXIV Respublika elmi konfransı, – Bakı: – 17 may, – 2024, – s. 56-57.
  27. Kərimli, F.K., Niftiyev, N.N., Daşdəmirov, A.O. FeIn<sub>2</sub>S<sub>4</sub> birləşməsinin elektrik sahəsində elektrik keçiriciliyinin tədqiqi // «Fizika və Astronomiya problemləri» XXIV Respublika elmi konfransının materialları, – Bakı: – 17 may, – 2024, – s. 68-69.
  28. Niftiyev, N.N. Electrical properties of FeGa<sub>0.4</sub>In<sub>1.6</sub>Se<sub>4</sub> at alternating current / N.N.Niftiyev, A.O.Dashdemirov, F.M.Mamedov [et al.] // Surface Engineering and Applied Electrochemistry, – 2024. Mar.; v. 60, № 6, – p. 821-825.

29. Niftiyev, N.N. Frequency dispersion of dielectric coefficients of  $\text{MnGaInTe}_4$  crystals / N.N.Niftiyev, A.O.Dashdemirov, F.M.Mammadov [et al.] // *Semiconductor Physics, Quantum Electronics & Optoelectronics*, – 2024. Jun.; v. 27, № 2, – p. 189-193.
30. Daşdəmirov, A.O., Əkərbərov, A.S. GeS laylı monokristalından alternativ enerji mənbəyi kimi istifadə olunma perspektivləri // «İnnovativ ekosistemlərin inkişafında universitetlərin rolu», – Gəncə: ATU, – 5 – 6 noyabr, – 2024, – s. 127-129.
31. Daşdəmirov, A.O., Əkərbərov, A.S. Radiasiya şüalarının GaS laylı monokristalının fotoelektrik spektrinə təsiri // «Fizikanın aktual problemləri» Respublika elmi konfransı, – Bakı: ADPU, – 29 noyabr, – 2024, – s. 28-30.
32. Dashdemirov, A.O., Alekperov, A.S. Influence of Rare Earth Metals on Electrophysical Properties of GeS Layered Monocrystalline // 8<sup>th</sup> International Conference Modern Trends in Physics, – Bakı: BSU, – 30 November-1 December, – 2023. – p. 90-91.
33. Dashdemirov, A.O. Heat flux and mass effect in the  $\text{Cu}_{2-x}\text{Tm}_x\text{Se}$  system at high temperatures / A.O.Dashdemirov, Y.I.Aliyev, S.R.Azimova [et al.] // *Advanced Physical Research*, – 2025. Jan.; v. 7, № 1, – p. 111-117.
34. Niftiyev, N.N. Some optoelectronic properties of  $\text{FeGaInSe}_4$  crystals under laser excitation / N.N.Niftiyev, F.M.Mammadov, A.O.Dashdemirov [et al.] // *Semiconductor Physics, Quantum Electronics & Optoelectronics*, – 2025. Mar.; v. 28, № 1, – p. 33-36.
35. Samadov, S. Study of germanium sulfide thin films by doppler broadening spectroscopy / S.Samadov, A.Sidorin, A.Dashdemirov [et al.] // *Indian Journal of Physics*, – 2025. Jul.; – pp. 1-6.

The defense of the dissertation will be held on 24 October 2025 at 15<sup>00</sup>- at the meeting of the Dissertation Council ED 2.19 of Supreme Attestation Commission under the President of the Republic of Azerbaijan operating at Baku State University.

Address: AZ 1148, 23, Z. Khalilov str., Baku, Baku State University.

The dissertation is accessible at the Baku State University library.

The electronic versions of dissertation and its abstract are available on the official website of Baku State University.

The abstract was sent to the required addresses "18" September 2025.

A handwritten signature in blue ink, appearing to read "Shayda", with a long horizontal stroke extending to the left and a large loop on the right.

**Signed for print: 16.09.2025**  
**Paper format: A5 (60x84 1/16)**  
**Volume: 52846 char.**  
**Number of hard copies: 20 copies**